Second-harmonic generation of thermally poled silver doped sodo-borophosphate glasses

Evelyne Fargin, Jérémy Soulié, Thierry Cardinal, Michel Lahaye, Vincent Rodriguez, Michel Couzi, Frédéric Adamietz

Second-harmonic generation of thermally poled silver doped sodo-borophosphate glasses

Evelyne Fargin,[1] Jérémy Soulié,[1,2] Thierry Cardinal,[1] Michel Lahaye,[1] Vincent Rodriguez,[2,a)] Michel Couzi,[2] and Frédéric Adamietz[2]
[1]*Institut de Chimie de la Matière Condensée de Bordeaux-UPR 9048 CNRS, Université de Bordeaux, Avenue du Dr. Schweitzer, 33608 Pessac Cedex, France*
[2]*Institut des Sciences Moléculaires, UMR 5255 CNRS, Université de Bordeaux, 351 cours de la Libération, 33405 Talence Cedex, France*

(Received 24 July 2008; accepted 10 November 2008; published online 26 January 2009)

Sodium niobium borophosphate glass, with a composition of $0.58(0.95NaPO_3+0.05Na_2B_4O_7)+0.42Nb_2O_5$, has been doped with monovalent silver ions. Second harmonic generation (SHG) has been obtained from the poling treatment of this sample. The second order nonlinearity from the anode side was estimated from an analysis of transmitted polarized Maker-fringe patterns. Thanks to the original Maker fringe simulations, a value of 3 pm/V is obtained with the silver doped glass that unambiguously scales an enhancement of ~35% with respect to the nondoped glass susceptibility. For both glasses, the nonlinear layer is found to be sodium-depleted up to 4 μm inside the anode, in accordance with quantitative energy dispersive x-ray spectroscopy characterizations. This comparative study indicates complex space-charge-migration processes during the poling treatment. The relative enhancement of the SHG signal of the silver doped glass is correlated with the increase in its linear susceptibility. © *2009 American Institute of Physics*. [DOI: 10.1063/1.3054182]

I. INTRODUCTION

The development of optical communication technologies created an important interest in materials with nonlinear optical (NLO) properties. The ideal material should combine large nonlinear coefficient, good optical quality, and low optical loss. It is now well known that, in glasses, a thermal poling treatment may induce a second harmonic response suitable for electro-optical applications. Myers *et al.*[1] and Mukherjee *et al.*[2] proposed a model where the $\chi^{(2)}$ signal induced by the thermal poling process originates from a third order nonlinear susceptibility $\chi^{(3)}$ of the material through the remaining internal electric field E_{int}, i.e, $\chi^{(2)}=3\chi^{(3)}E_{int}$, efficient in a layer of a few micrometers under the surface in contact with the anode or either from a structural polar reorganization of the entities. Recent studies show surprisingly that glasses with large concentration of charge carriers may have significant quadratic optical nonlinearity after thermal poling.[3–6] For poled sodium niobium borophosphate glasses, in the particular system $(1-x)(0.95NaPO_3+0.05Na_2B_4O_7)+xNb_2O_5$, promising results have already been obtained in a surface layer of 3–5 μm depleted on sodium, the second order optical susceptibility $\chi^{(2)}$ increasing significantly with niobium content to reach 4–5 pm/V for $x=0.47$.[7,8] The crystallization in such glass systems was also investigated.[9] Silver ions have been shown to be nucleating agents in glasses.[10] In order to control further crystallization of dielectric nanoparticles in the poled glass, silver ions were here introduced in the glass composition. The idea was here to study silver doping using standard glass melting technique on the glass thermal and optical behavior and on $\chi^{(2)}$ efficiency after poling. In a first step the study of silver ions behavior under field during the poling process is presented here.

II. EXPERIMENTAL SECTION AND RESULTS

A. Glass synthesis, characterization, and thermal poling

Bulk samples with molar compositions $[0.58(0.95NaPO_3+0.05Na_2B_4O_7)+0.42Nb_2O_5]$ (called BPN42) and $0.995[0.58(0.95NaPO_3+0.05Na_2B_4O_7)+0.42Nb_2O_5]+0.005Ag_2O$ (called BPN42Ag) were elaborated by a classical glass melting technique. High purity reagent powders of $NaPO_3$, $Na_2B_4O_7$, Nb_2O_5, and $AgNO_3$ were mixed and grounded, poured in a platinum crucible, and melted at a temperature of 1300 °C. Silver has been incorporated using part of undoped glasses and remelting. For the silver doped composition, a pretreatment of mixed undoped glass and silver nitrate has been carried out for total departure of NO_2 (700 °C during 3 h). The melts were poured and quenched in a brass preform. Differential scanning calorimetry (heating rate of 10 °C/min) allowed determining of the glass transition temperature and the crystallization temperatures for each composition (Fig. 1).

The glasses formed were annealed under air, 30 °C below the glass transition temperature. Transparent samples with 1 cm^2 surface and 1 mm thick were cut and polished on both sides. Each glass was then submitted to the poling process after being sandwiched between polished *n*-doped silicon wafer at the anode and thin borosilicate glass plate at the cathode, then pressed on both sides by the electrodes and heated to 230 °C. This temperature was chosen to make sure

a)Author to whom correspondence should be addressed. Electronic address: vincent.rodriguez@u-bordeaux1.fr.

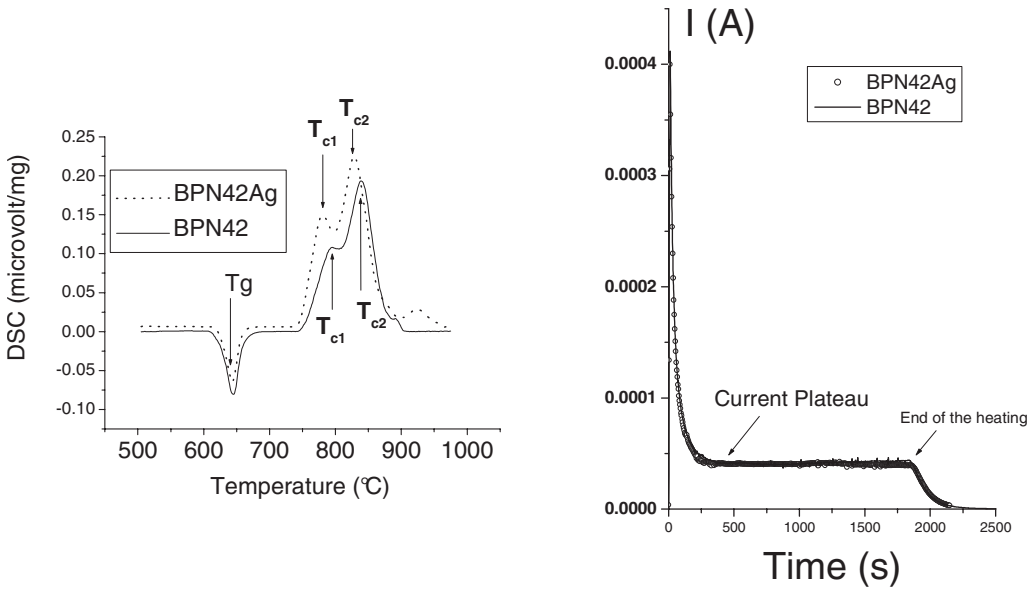

FIG. 1. Left: differential scanning calorimetry measurements that determine the glass transition temperatures and the crystallization temperatures for each glass. Right: electrical current (in milliamperes) as a function of temperature during the poling treatment of BPN45 and BPN45Ag using the same poling conditions.

poling is efficient according to a previous study.[7] The current was simultaneously registered in order to control the end of ions migration obtained when the current reaches a plateau (Fig. 1). The applied voltage was 1.1 kV during 1800 s. Then samples were cooled down before the external voltage was removed.

B. Quantitative and micro-Raman analyses

Energy dispersive x-ray spectroscopy (EDS) allowed the identification of the elemental composition of the studied samples. Further quantitative analyses were performed by using electron probe microanalysis combined with wavelength dispersive spectrometer (WDS). For these analyses, the precision was about 1% (in at. %) for all abundant elements (Na, P, Nb) and approximately 10% for Ag. At first, the stoichiometry of the BPN42Ag glass was controlled. Then the atomic concentrations profiles of silver, phosphorus, niobium, and sodium ions were computed after poling along the cross section of the poled glass zone close to the anode side (standard spatial resolution of 1 μm). The results are given in Fig. 2 where concentrations are reported as atomic percentage, ensuring the stoichiometry with oxygen atoms on the basis of Nb_2O_5, Na_2O, P_2O_5, and ruling out B_2O_3 from the composition since B atoms cannot be analyzed with this method. These results are quite comparable to previously published profiles obtained for BPN42 glass composition,[7,8] considering N, P, and Nb at. %.

The Raman spectra were recorded with a Labram confocal micro-Raman instrument (Horiba/Jobin-Yvon) (typical resolution of 2 cm^{-1}) in the backscattering geometry at room temperature. The spectrophotometer includes a holographic Notch filter for Rayleigh rejection, a microscope equipped with $\times 100$ objectives, and a charge couple device (CCD) detector. The 514.5 nm emission line of an argon ion laser was used for excitation. Spectra were recorded at different areas of the poled glasses (Fig. 3).

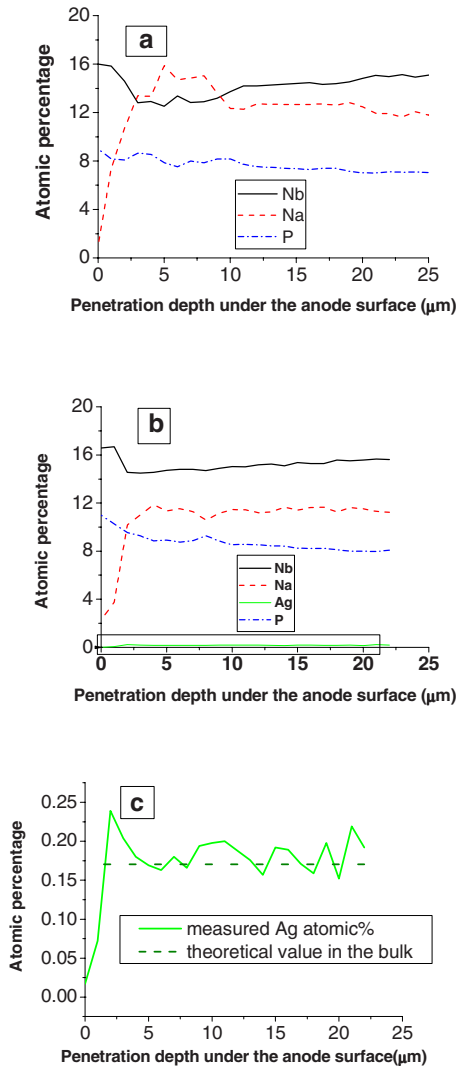

FIG. 2. (Color online) Atomic percentage of sodium, silver, phosphorus, and niobium ions profiles, close to the anode interface after poling, measured by quantitative EDS for (a) BPN42 and [(b) and (c)] BPN42Ag, where a focus on the silver ions profile is plotted.

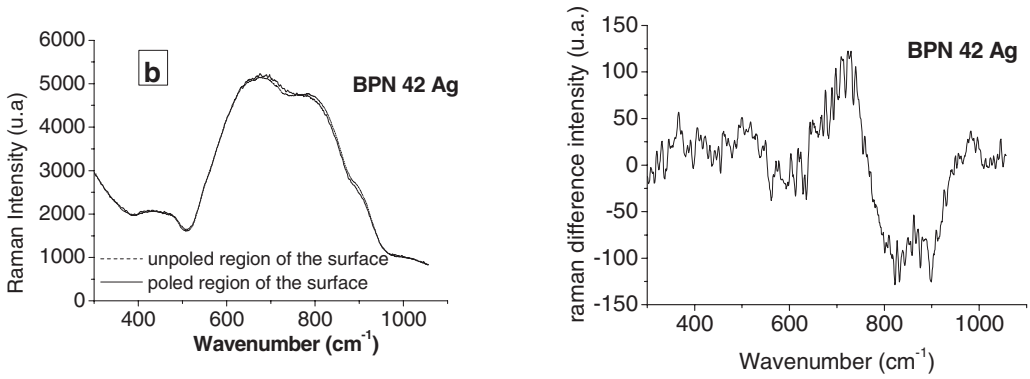

FIG. 3. Left: confocal micro-Raman spectra inside and outside the poled area of BPN42Ag. Right: corresponding Raman difference spectra.

C. Linear optical characterizations

The transmission spectra in the UV-visible region of unpoled BPN42 and BPN42Ag polished samples were recorded to compare the effect of silver doping. Both samples exhibit a perfect transmission, from 2500 nm, in the near-infrared (NIR) region, to the cutoff wavelength, approximately 350 nm (Fig. 4). A slight bathochromic shift is observed for the silver doped glass.

Linear refractive indices at 1064 and 532 nm were previously measured using the Brewster angle reflection method over the $\pm[10°;80°]$ wide θ range, inside and outside the poled region, for both poled BPN42 and BPN42Ag glasses (Table I). These preliminary linear optical measurements are also a useful first step that enforces the accuracy of the SHG simulations since they give the coherence length, $L_c = \lambda/(4|n_\omega - n_{2\omega}|)$, of thin NLO layers, which is difficult to estimate with SHG experiments alone.

D. Measurements of second harmonic generation

Second harmonic generation (SHG) measurements in transmission mode were performed on poled BPN42 and BPN42Ag samples using a neodymium-doped yttrium aluminum garnet laser ($\lambda = 1064$ nm, 20 Hz, 20 ns pulses). For both samples, a typical energy of 150 μJ was necessary to record the harmonic transmitted *pp* and *sp* polarized Maker fringes patterns by varying the incidence angle.

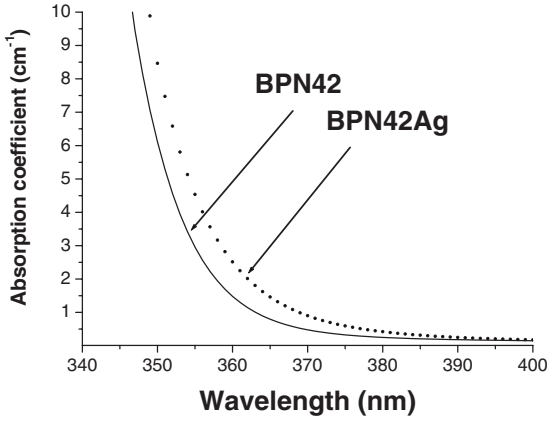

FIG. 4. Absorbance spectra (transmission) of the glasses before the poling treatment.

Actually, the sensitivity and selectivity of the SHG technique becomes less effective when studying thin films, surfaces, or interfaces, with the traditional Maker fringe technique (scanning of the incident angle with fixed incident polarization). Thus in thin film SHG experiments, continuous polarization scans of the input beam at a fixed incidence angle can also be performed as it is depicted in Fig. 5. The fundamental beam, initially polarized out of the plane of incidence (*s*) is passed through a combination of a rotating half wave plate and a fixed quarter wave plate (vertical fast axis) to address all possible polarizations, from linear to elliptical and to circular polarization. The incident beam is focused on the sample at a fixed incident angle and transmitted second harmonic light is resolved into components polarized parallel (*p*) and perpendicular (*s*) to the horizontal plane of incidence. Here in Fig. 5, the second-harmonic intensity is recorded versus the rotation angle of the half wave plate (angle ψ).

Hence, polarization scans (as a function of the half wave plate angle ψ) have been performed at a fixed incidence angle of 45° to improve the quality of the SHG measurements. Such SHG polarization scans considered together with classical *pp*- and *sp*-polarized angular scans give indeed trustful and accurate results when studying thin NLO films or interfaces (see e.g., Ref. 11). The four experimental patterns were simulated together following a general optical transfer matrix procedure described elsewhere.[12,13] For both poled transparent glasses, the NLO layer is located at the anode interface and the corresponding contracted 3×6 SHG tensor contains two related nonzero components $\chi_{33}^{(2)} = 3\chi_{31}^{(2)}$.[3,4] Experimental and simulated SHG signals of the BPN42Ag poled sample are plotted in Fig. 6 and the corresponding SHG results are also gathered in Table I.

III. DISCUSSION

The DSC signal, collected for both glasses, exhibits similar shapes with an endothermic signal corresponding to the glass transition and two exothermic features at higher temperature corresponding to the crystallization phenomena. Temperatures of endothermic and exothermic effects correspond, respectively, to glass transitions (T_g) and beginning of crystallization processes (T_{c1} and T_{c2}).

First crystallization maximum corresponds to crystallization of the phase $Na_{1.1}Nb_{2.98}O_8$ for all sodium containing

TABLE I. Refractive indices, SHG susceptibility, and thickness of the NLO layer of BPN42 and BPN42Ag.

	$n_{1064\ nm}$ (± 0.01)		$n_{532\ nm}$ (± 0.01)		$\chi^{(2)}_{33}$	Thickness
	Unpoled area	Poled area	Unpoled area	Poled area	(± 0.1 pm/V)	(± 0.1 μm)
BPN42	1.84	1.72	1.92	1.75	2.2	4.0
BPN42Ag	2.06	1.78	2.12	1.84	3.0	4.0

glasses. Crystallization behaviors of sodium niobium borophosphate glasses and structural particularities of the $Na_{1.1}Nb_{2.98}O_8$ phase were studied earlier.[9] The second peak has been attributed to crystallization of the $Na_4Nb_8P_4O_{32}$ phase.[9] No significant effect of the silver addition on glass transition temperature T_g can be noticed according to the measurement precision, but an increase in the slope of the curve from the beginning of the crystallization to the first maxima T_{c1} is observed. As previously pointed out by Glebov[10] for another glass composition, here, silver ions can also be considered as a nucleating agent accelerating the first crystallization exothermic phenomenon.

The UV-visible-NIR spectra confirm the perfect and wide range of transmissions for both BPN42 and BPN42Ag samples. The mean cutoff wavelength is estimated at (350 ± 5) nm in the transmission mode for 1 mm thick plate glasses. Note that the bathochromic shift observed when introducing silver is in agreement with a stronger index of refraction (see Table I, unpoled area). If we focus now on the structural features of the samples, the Raman spectra of the poled NLO layer at the anode interface exhibit indeed small differences that completely disappear 4 μm far from this interface. The 500–1000 cm^{-1} large band is usually attributed to Nb–O bonds in the glass,[8,14,15] and the relative intensities of the three main components of this band have been clearly correlated with an enhancement of third order NLO susceptibilities observed for large concentrations of niobium. This band is globally narrowed in the poled zone. Features appear in the difference spectra, which have already been observed and analyzed in the poled BPN42 glass composition.[16] Thus, no clear effect of Ag doping is revealed from the Raman spectra and also no obvious difference in the local structure of unpoled and poled glasses can be evidenced.

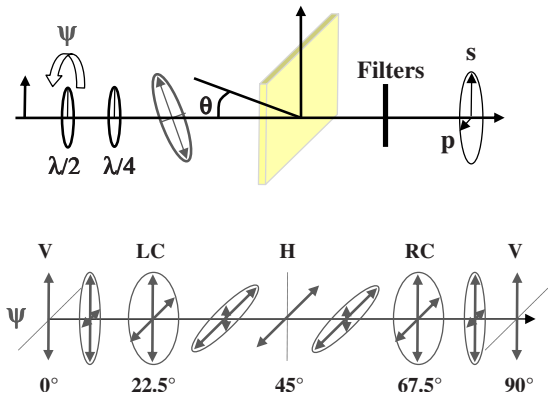

FIG. 5. (Color online) Top: scheme of a SHG experiment in transmission with a continuous polarization scan. Bottom: the combination of a rotating half waveplate (with angle ψ) and a fixed quarter waveplate (vertical fast axis) address all possible polarizations, from linear to elliptical and circular polarization.

WDS quantitative studies of P, Nb, Na, and Ag elements on the cross section of the two BPN42Ag and BPN42 glasses in their poled regions are comparable with the previous analysis of a poled BPN42 glass.[7,8] For both glasses, a quite complete depletion of sodium under the anode surface is observed and the bulk concentration is recovered 3–5 μm after the anode surface (the spatial resolution being around 1 μm for these measurements). However, in BPN42Ag, inside the Na^+ depleted layer, a net depletion of silver ions is observed in a first 2–3 μm thick sublayer located at the anode interface. After each depleted layer (Na^+ and Ag^+), a slight excess of sodium and silver ions seems to appear before the bulk concentration of each ion is recovered. Such features (accumulation of ions along a few micrometers) have already been observed;[17] however here, further precise studies must be undertaken to confirm this point. As a partial conclusion, clearly the nonlinear zone at the anode can be described as a first layer free from sodium and silver ions and of a second layer still without sodium ions but now containing silver ions. The number of silver ions migrating during poling is very low with respect to sodium ions and probably negligible since we observe identical poling current curves and plateau in Fig. 1. The total space charge corresponding to the migration of ions obtained from the integration of the curve above the plateau gives $\sim 1.7 \times 10^8$ C m^{-3} (considering the migration normalized to the electrode surface and a total depleted layer 4 μm thick). We estimate the density number of migration ions around 10^{27} ions/m^3, which is in good agreement with the density number of sodium ions (when neglecting the number of silver ions in BPN42Ag) for both glasses that equals 6×10^{26} ions/m^3.

Thermal poling in both BPN42 and BPN42Ag does induce an efficient nonlinear response from the anode interface through ~ 4 μm inside the glass bulk as confirmed both by WDS quantitative analysis and SHG analyses. Actually, concerning the SHG treatment of BPN42Ag, we only considered one NLO layer with a thickness of 4 μm that corresponds to the Na^+ and Ag^+ depleted area. Indeed, it is not expected that introducing two NLO sublayers, with the first one corresponding to the depletion of both Na^+ and Ag^+ ions and the second one to the depletion of Na^+ ions, would modify significantly the NLO response. The corresponding mean susceptibility for a whole unique layer in BPN42Ag is $\chi^{(2)}_{33} = 3$ pm/V, while it is $\chi^{(2)}_{33} = 2.2$ pm/V for BPN42. On one hand, these large values have previously been explained by a

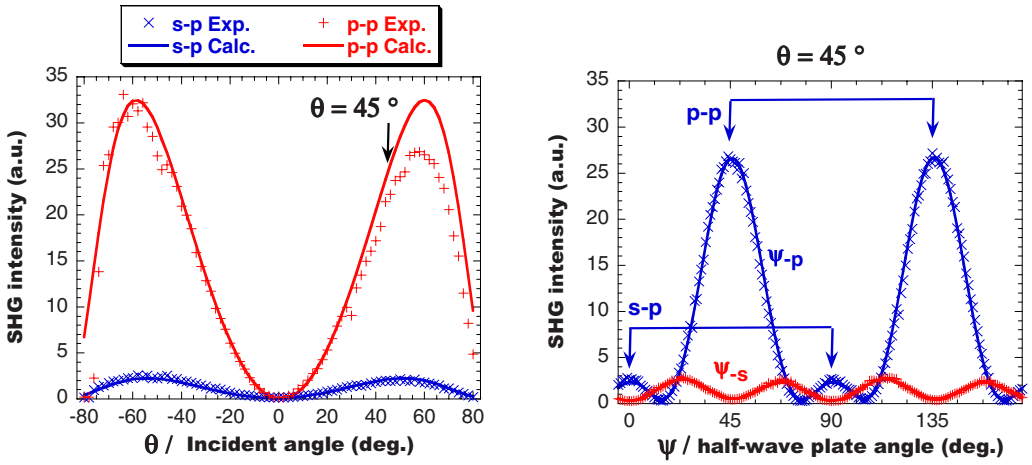

FIG. 6. (Color online) Experimental (crosses) and calculated (solid lines) transmitted polarized Maker fringe patterns obtained for the BPN42Ag glass sample. Left: the polarized geometries *pp* and *sp* correspond to either a *p* (in plane) or *s* (out of plane) polarized incident beam, respectively, and a *p* polarized harmonic signal. Right: continuous polarization scan patterns obtained at an incident angle of 45°, where the harmonic signal *p*- (*s*-) polarized corresponds to ψ-*p* (ψ-*s*).

large ionic conductivity[18] that triggers a strong (and stable) space charge during (and after) the poling. This effect combined with the high $\chi^{(3)}$ response of the glassy material, directly correlated with the extent of niobium in the glass,[7,8] explains the resulting second order NLO response. On the other hand, when comparing the susceptibilities of the two glasses, which have been identically treated, the inclusion of silver ions contributes by increasing the global SHG signal up to ~35%. In fact, the relative enhancement of the second-order susceptibility of BPN42Ag is indirectly connected to the bathochromic effect observed through the cutoff wavelength, i.e., it comes from pure linear optical effects (close to resonance) as it is demonstrated below.

Invoking a simple description of the motion of electrons in response to an electric field, the second-order susceptibility can be expressed in terms of the product of linear susceptibilities,[19]

$$\chi^{(2)}(2\omega) \propto \chi^{(1)}(2\omega)[\chi^{(1)}(\omega)]^2. \quad (1)$$

Following Eq. (1), an increase in the linear susceptibilities will also increase the second order susceptibility. As a consequence, susceptibilities ratios of BPN42Ag versus BPN42 using Eq. (1) are expected to be equal.

First, from the data given in Table I, the ratio of the NLO susceptibilities is

$$\chi^{(2)}_{\mathrm{BPN42Ag}}(2\omega)/\chi^{(2)}_{\mathrm{BPN42}}(2\omega) = 3.0/2.2 \approx 1.4. \quad (2)$$

Second, since $\chi^{(1)}(\omega)$ is related to the refractive index n_ω and the high frequency dielectric constant ε_ω, by $n_\omega^2 = \varepsilon_\omega = 1 + 4\pi\chi^{(1)}(\omega)$, we can evaluate all the $\chi^{(1)}$ terms from the data given in Table I and we obtain

$$\chi^{(1)}_{\mathrm{BPN42Ag}}(2\omega)[\chi^{(1)}_{\mathrm{BPN42Ag}}(\omega)]^2/\chi^{(1)}_{\mathrm{BPN42}}(2\omega)[\chi^{(1)}_{\mathrm{BPN42}}(\omega)]^2 = 11.2/7.9 \approx 1.4. \quad (3)$$

As expected, we clearly see that Eqs. (2) and (1) are equal, confirming that the addition of silver increases the global linear and NLO susceptibilities because it increases the electronic polarizability of the material. This result also indicates that no plasmon enhancement effects due to silver aggregation are evidenced.

IV. CONCLUSION

This work compared the SHG efficiency of a poled sodium niobium borophosphate glass, without or doped with silver. Sodium and sodium/silver ion concentration profiles under the anode have been computed for both glass compositions and compared. For the undoped and doped glasses, the sodium depletion zone thicknesses are identical. The poling treatment involves the simultaneous migration of sodium and silver ions in the silver doped glass. However, the silver depletion zone thickness obtained in the doped glass is not as large as the sodium depletion zone. Such an effect may be connected to the activation energies of these ions mobilities in the glass, which are very close, and the fact that, in these niobium borophosphate glasses, sodium ions move faster. A bathochromic increase in the cutoff wavelength is observed after poling in the silver doped glass. The increase in the linear and nonlinear susceptibilities with the addition of silver results from this bathochromic effect and is at the origin of the enhancement of the quadratic susceptibility.

ACKNOWLEDGMENTS

This work was supported by Région Aquitaine, Agence Nationale de la Recherche (project "Research and Education in Glass and Laser Interaction Science," Contract No. ANR-05-BLAN-0212-01).

[1] R. A. Myers, N. Mukherjee, and S. R. J. Brueck, Opt. Lett. **16**, 1732 (1991).
[2] N. Mukherjee, R. A. Myers, and S. R. J. Brueck, J. Opt. Soc. Am. B **11**, 665 (1994).
[3] F. C. Garcia, I. C. S. Carvalho, E. Hering, W. Margulis, and B. Leshe, Appl. Phys. Lett. **72**, 3252 (1998).
[4] H. An and S. Flemming, Appl. Phys. Lett. **89**, 181111 (2006); J. Opt. Soc. Am. B **23**, 2303 (2006).
[5] C. R. Mariappan and B. Roling, Solid State Ionics **179**, 671 (2008).
[6] S. Ukon, Y. Tsujiie, S. Murai, K. Fujita, and K. Tanaka, Adv. Mater. Res.

39–40, 247 (2008).
[7]M. Dussauze, E. Fargin, M. Lahaye, V. Rodriguez, and F. Adamietz, Opt. Express **13**, 4064 (2005).
[8]M. Dussauze, E. Fargin, A. Malkho, V. Rodriguez, T. Buffeteau, and F. Adamietz, Opt. Mater. (Amsterdam, Neth.) **28**, 1417 (2006).
[9]A. Malakho, M. Dussauze, E. Fargin, B. Lazoriak, V. Rodriguez, and F. Adamietz, J. Solid State Chem. **178**, 1888 (2005).
[10]L. B. Glebov, Opt. Mater. (Amsterdam, Neth.) **25**, 413 (2004).
[11]V. Rodriguez, G. Koeckelberghs, and T. Verbiest, Chem. Phys. Lett. **450**, 76 (2007).
[12]V. Rodriguez and C. Sourisseau, J. Opt. Soc. Am. B **19**, 2650 (2002).
[13]V. Rodriguez, J. Chem. Phys. **128**, 064707 (2008).
[14]T. Cardinal, E. Fargin, G. Le Flem, and S. Leboiteux, J. Non-Cryst. Solids **222**, 228 (1997).
[15]A. A. Lipovskii, D. K. Tagantsev, A. A. Vetrov, and O. V. Yanush, Opt. Mater. (Amsterdam, Neth.) **21**, 749 (2003).
[16]M. Dussauze, E. Fargin, V. Rodriguez, A. Malakho, and E. Kamitsos, J. Appl. Phys. **101**, 083532 (2007).
[17]T. G. Alley, S. R. J. Brueck, and R. A. Myers, J. Non-Cryst. Solids **242**, 165 (1998).
[18]M. Dussauze, O. Bidault, E. Fargin, M. Maglione, and V. Rodriguez, J. Appl. Phys. **100**, 034905 (2006).
[19]R. W. Boyd, *Nonlinear Optics*, 2nd ed. (Academic, San Diego, 2003).